Mathematical Modelling and Analysis
Volume 22 Number 3, May 2017, 271–282
https://doi.org/10.3846/13926292.2017.1306809

Publisher: Taylor&Francis and VGTU
http://www.tandfonline.com/TMMA
ISSN: 1392-6292
eISSN: 1648-3510

Numerical Method for Electromagnetic Wave Propagation Problem in a Cylindrical Inhomogeneous Metal Dielectric Waveguiding Structures

Eugene Smolkin

Penza State University
Krasnaya street 40, 440026 Penza, Russia
E-mail(*corresp.*): e.g.smolkin@hotmail.com

Received August 22, 2016; revised February 19, 2017; published online May 15, 2017

Abstract. The propagation of monochromatic electromagnetic waves in metal circular cylindrical dielectric waveguides filled with inhomogeneous medium is considered. The physical problem is reduced to solving a transmission eigenvalue problem for a system of ordinary differential equations. Spectral parameters of the problem are propagation constants of the waveguide. Numerical results are found with a projection method. The comparison with known exact solutions (for particular values of parameters) is made.

Keywords: Maxwell's equations, boundary value problem, projection method, numerical method.

AMS Subject Classification: 78M25.

1 Introduction

A large class of vector electromagnetic problem concerns electromagnetic wave propagation. In radioengineering and electronics the use becomes waveguide structures of complex cross-sections and with inhomogeneous filling require the construction of mathematical models of the propagation of electromagnetic waves in such structures. It becomes necessary to study a new broad class of problems in electrodynamics, characterized by boundaries with delete, give rise to complex geometry, surfaces, uneven dielectric filling and the presence of thin metal ribs (plates) in the structure. The primary goal here is to construct a numerical method to determine the spectrum of normal electromagnetic waves that propagate in such structures.

The study of the wave propagation in a waveguide filled with inhomogeneous medium are arise a boundary eigenvalue problems for systems of elliptic equations with discontinuous coefficients. On the surfaces of discontinuity are

set additional conditions, called transmission conditions. In the simplest formulations the spectral parameter is present only in the equations, and is not included in the transmission conditions. However, in rather complex models a spectral parameter is included not only in the equation, but also in the transmission conditions.

This class of problems has been developed for many years [3,7,12]. The main attention was paid to practical outcomes of the calculation of the characteristics of the main mode of waves which has a greatest interest from the physical point of view, as well as several higher modes. Numerical methods for calculating the parameters of various types of waveguide structures are described in the monographs and review papers [1,4,6,15]. However, it should be said that most of the methods applied to homogeneous waveguides, are not common and are difficult to implement and apply for specific inhomogeneous structures.

In this work the wave propagation in inhomogeneous metal-dielectric cylindrical waveguides is studied numerically using the modification of the projection methods. We consider two types of waveguides: a two-layer dielectric waveguide covered by metal where one of the layers is filled with nonlinear medium and a perfectly conducting cylinder covered by a nonlinear dielectric layer. The obtained numerical results are compared with the data available in the linear theory.

2 Statement of the problem

Consider three-dimensional space $\mathbb{R}^3$ with a cylindrical coordinate system $O\rho\varphi z$ filled with isotropic medium having constant permittivity $\varepsilon = \varepsilon_0$ ($\varepsilon_0 > 0$ is the permittivity of free space), and constant permeability $\mu = \mu_0$ (where $\mu_0 > 0$ is the permeability of free space).

A metal dielectric circular cylindrical waveguide Σ filled with inhomogeneous medium is placed parallel to the axis Oz.

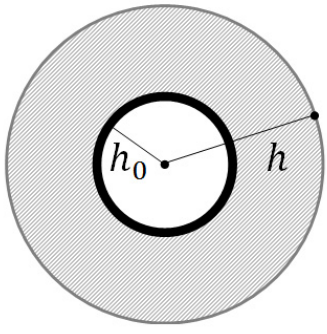

Figure 1. The perfectly conducting cylinder covered by the dielectric layer.

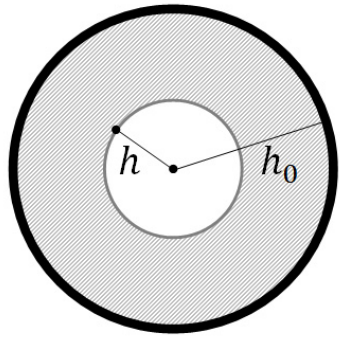

Figure 2. The circular hollow metallic layered waveguide.

In Figure 1 a perfectly conducting cylinder covered by a dielectric layer, known as Goubau line (GL) is shown. In Figure 2 a circular hollow metallic

layered waveguide (HW) is shown.

We will consider monochromatic waves

$$\mathbf{E}e^{-i\omega t} = e^{-i\omega t}\,(E_\rho, E_\varphi, E_z)^T\,, \quad \mathbf{H}e^{-i\omega t} = e^{-i\omega t}\,(H_\rho, H_\varphi, H_z)^T\,,$$

where $(\,\cdot\,)^T$ denotes the transpose operation. Each component of the field $\mathbf{E}$, $\mathbf{H}$ is a function of three spatial variables. Complex amplitudes of the electromagnetic field $\mathbf{E}, \mathbf{H}$ satisfy the Maxwell equations

$$\begin{cases} \mathrm{rot}\mathbf{H} = -\mathrm{i}\omega\varepsilon\mathbf{E}, \\ \mathrm{rot}\mathbf{E} = \mathrm{i}\omega\mu\mathbf{H}, \end{cases} \tag{2.1}$$

subject to the following boundary conditions. The tangential components of the electric field vanish on the metal surface $\rho = h_0$; tangential field components are continuous on the media interface $\rho = h$; the complex amplitudes obey the radiation condition at infinity: the electromagnetic field decays as $O(|\rho|^{-1})$ when $\rho \to \infty$. The dielectric permittivity inside a ring (segment $[h_0,\ h]$) is described by a smooth function $\varepsilon\,(\rho)$.

The surface waves propagating along the axis Oz of the waveguide Σ have the form [11]

$$\begin{aligned} E_\rho &= \mathrm{E}_\rho(\rho)e^{im\varphi+i\gamma z}, \quad & H_\rho &= \mathrm{H}_\rho(\rho)e^{im\varphi+i\gamma z}, \\ E_\varphi &= \mathrm{E}_\varphi(\rho)e^{im\varphi+i\gamma z}, \quad & H_\varphi &= \mathrm{H}_\varphi(\rho)e^{im\varphi+i\gamma z}, \\ E_z &= \mathrm{E}_z(\rho)e^{im\varphi+i\gamma z}, \quad & H_z &= \mathrm{H}_z(\rho)e^{im\varphi+i\gamma z}, \end{aligned} \tag{2.2}$$

where γ is the real propagation constant (spectral parameter of the problem) and m is an angular integer parameter (which assumed to be known). In what follows we often omit the arguments of functions when it does not lead to misunderstanding.

3 Differential equations

Substituting $\mathbf{E}$ and $\mathbf{H}$ with components (2.2) into equations (2.1), we obtain

$$\begin{cases} i\dfrac{m}{\rho}H_z - i\gamma H_\varphi = -i\omega\varepsilon E_\rho, & i\gamma H_\rho - H_z' = -i\omega\varepsilon E_\varphi, \\ \dfrac{1}{\rho}(\rho H_\varphi)' - \dfrac{im}{\rho}H_\rho = -i\omega\varepsilon E_z, & i\dfrac{m}{\rho}E_z - i\gamma E_\varphi = i\omega\mu H_\rho, \\ i\gamma E_\rho - E_z' = i\omega\mu H_\varphi, & \dfrac{1}{\rho}(\rho E_\varphi)' - \dfrac{im}{\rho}E_\rho = i\omega\mu H_z, \end{cases} \tag{3.1}$$

where the prime denotes differentiation w.r.a ρ.

Expressing the functions E_ρ,E_φ, H_ρ and H_φ through E_z and H_z from the 1st, 2nd, 4th and 5th equation of system (3.1), we find

$$\begin{aligned} E_\rho &= \frac{i\gamma\rho E_z' - m\omega\mu H_z}{\rho(\omega^2\mu\varepsilon - \gamma^2)}, \quad & H_\rho &= \frac{m\omega\varepsilon E_z + i\gamma\rho H_z'}{\rho(\omega^2\mu\varepsilon - \gamma^2)}, \\ E_\varphi &= -\frac{\gamma m E_z + i\omega\mu\rho H_z'}{\rho(\omega^2\mu\varepsilon - \gamma^2)}, \quad & H_\varphi &= \frac{i\omega\varepsilon\rho E_z' - \gamma m H_z}{\rho(\omega^2\mu\varepsilon - \gamma^2)}. \end{aligned}$$

Substituting the expressions for E_ρ, E_φ, H_ρ and H_φ into the 3rd and 6th equations of system (3.1) and introducing the notation $u_{\text{E}} := iE_z(\rho)$, $u_{\text{M}} := H_z(\rho)$, we obtain

$$\begin{cases} L_{\text{E}}u_{\text{E}} := \dfrac{d}{d\rho}\Big(p_{\text{E}}\dfrac{du_{\text{E}}}{d\rho}\Big) - q_{\text{E}}u_{\text{E}} = fu_{\text{M}}, \\ L_{\text{M}}u_{\text{M}} := \dfrac{d}{d\rho}\Big(p_{\text{M}}\dfrac{du_{\text{M}}}{d\rho}\Big) - q_{\text{M}}u_{\text{M}} = fu_{\text{E}}, \end{cases} \tag{3.2}$$

where

$$p_{\text{E}} = \frac{\omega\varepsilon\rho}{k^2}, \quad p_{\text{M}} = \frac{\omega\mu\rho}{k^2}, \quad q_{\text{E}} = \frac{\omega\varepsilon}{\rho}\left(\frac{m^2}{k^2} - \rho^2\right),$$
$$q_{\text{M}} = \frac{\omega\mu}{\rho}\left(\frac{m^2}{k^2} - \rho^2\right), \quad f = -\frac{\gamma m}{k^4}\omega^2\mu\varepsilon', \quad k^2 = \omega^2\mu\varepsilon - \gamma^2.$$

Remark 1. For $m = 0$ system (3.2) splits into two independent equations, which corresponds to two independent wave propagation problems: for TE and TM guided waves. These problems are well studied (analytically and numerically) e.g. in [8, 9, 10, 13, 14, 16].

Outside the ring, where $\mu = \mu_0$ and $\varepsilon = \varepsilon_0$, system (3.2) takes the form of Bessel's equations

$$\rho(\rho u_{\text{E}}')' - \left(\rho^2 k_0^2 + m^2\right) u_{\text{E}} = 0,$$
$$\rho(\rho u_{\text{M}}')' - \left(\rho^2 k_0^2 + m^2\right) u_{\text{M}} = 0$$

with general solutions

$$u_{\text{E}} = C_1 I_m(k_0\rho) + C_2 K_m(k_0\rho), \quad u_{\text{M}} = C_3 I_m(k_0\rho) + C_4 K_m(k_0\rho), \tag{3.3}$$

where $k_0^2 = \gamma^2 - \omega^2\mu_0\varepsilon_0$, I_m is the modified Bessel function and K_m is the Macdonald function [5]. There $C_1, ..., C_4$ denote arbitrary constants.

For HW solutions (3.3) takes the form

$$u_{\text{E}} = C_1 I_m(k_0\rho), \ \ \rho < h, \quad u_{\text{M}} = C_2 I_m(k_0\rho), \ \ \rho < h, \tag{3.4}$$

where boundedness of the field at zero is taken into account.

For GL solutions (3.3) takes a form

$$u_{\text{E}} = C_1 K_m(k_0\rho), \ \ \rho > h, \quad u_{\text{M}} = C_2 K_m(k_0\rho), \ \ \rho > h, \tag{3.5}$$

where the radiation condition at infinity is taken into account.

4 Transmission conditions and transmission problem

Tangential components of the electromagnetic field are known to be continuous at the interface. In this case the tangential components are E_φ, E_z, H_φ and

H_z. Thus we obtain the following transmission conditions for u_{E} and u_{M}

$$\begin{aligned} u_{\text{E}}(h_0) = 0,\ u'_{\text{M}}(h_0) &= 0, \\ [u_{\text{E}}]|_{\rho=h} = 0,\ [u_{\text{M}}]|_{\rho=h} &= 0, \\ \gamma m \left[\frac{u_{\text{E}}}{k^2}\right]\Big|_{\rho=h} - [p_{\text{M}} u'_{\text{M}}]|_{\rho=h} &= 0, \\ \gamma m \left[\frac{u_{\text{M}}}{k^2}\right]\Big|_{\rho=h} - [p_{\text{E}} u'_{\text{E}}]|_{\rho=h} &= 0, \end{aligned} \tag{4.1}$$

where $[v]|_{\rho=s} = \lim\limits_{\rho\to s-0} v(\rho) - \lim\limits_{\rho\to s+0} v(\rho)$ is the jump of the limit values of the function at the point s.

The main problem (Problem P_m) is to find $\hat{\gamma}$ such that for a fixed value of angular parameter $m \neq 0$, there exist non-trivial functions $u_{\text{E}}(\rho;\hat{\gamma})$ and $u_{\text{M}}(\rho;\hat{\gamma})$ that satisfy system (3.2), transmission conditions (4.1), and inside the inhomogeneous layer they have the form (3.4) for HW or outside the layer the form (3.5) for GL.

5 Variation formulation

Let us give the variational formulation of the problem P_m. Using the first Green's formula, we obtain

$$\begin{aligned} \int_{h_0}^{h} vLud\rho &= \int_{h_0}^{h} v\left((pu')' - qu\right)d\rho \\ &= \int_{h_0}^{h} (pu'v)'\,d\rho - \int_{h_0}^{h} pu'v'd\rho - \int_{h_0}^{h} quvd\rho \\ &= pu'v|_{h_0}^{h} - \int_{h_0}^{h} pu'v'd\rho - \int_{h_0}^{h} quvd\rho. \end{aligned} \tag{5.1}$$

Taking into account the right-hand side of (3.2), we obtain

$$\int_{h_0}^{h} vLud\rho = \int_{h_0}^{h} fu^* vd\rho, \tag{5.2}$$

where u^* denotes a replacement by the rule $u^*_{\text{E}} = u_{\text{M}}$.

Let us consider the smooth test functions v_{E} and v_{M}.

Remark 2. We assume that the test functions v_{E} and v_{M} satisfy the following conditions

$$\begin{aligned} v_{\text{E}}(h_0) = 0,\ \ v_{\text{E}}(h) = 1, \\ v'_{\text{M}}(h_0) = 0,\ \ v_{\text{M}}(h) = 1, \end{aligned}$$

which coincide with conditions for functions u_{E} and u_{M} at the boundary h_0.

Multiplying the left and right sides of equations (3.2) by the test functions v_{E} and v_{M}, respectively, and applying (5.1) and (5.2), we obtain

$$p_{\text{E}}(h)u'_{\text{E}}(h)v_{\text{E}}(h) - \int_{h_0}^{h} p_{\text{E}}u'_{\text{E}}v'_{\text{E}}d\rho - \int_{h_0}^{h} q_{\text{E}}u_{\text{E}}v_{\text{E}}d\rho = \int_{h_0}^{h} fu_{\text{M}}v_{\text{E}}d\rho \tag{5.3}$$

and

$$p_{\text{M}}(h)u'_{\text{M}}(h)v_{\text{M}}(h) - \int_{h_0}^{h} p_{\text{M}}u'_{\text{M}}v'_{\text{M}}d\rho - \int_{h_0}^{h} q_{\text{M}}u_{\text{M}}v_{\text{M}}d\rho = \int_{h_0}^{h} fu_{\text{E}}v_{\text{M}}d\rho. \tag{5.4}$$

From (4.1) we determine $p_{\text{E}}u'_{\text{E}}$ and $p_{\text{M}}u'_{\text{M}}$ at the point h

$$\begin{aligned} p_{\text{E}}(h)u'_{\text{E}}(h) &= \gamma m\left(\frac{1}{k^2(h)} + \frac{1}{k_0^2}\right)u_{\text{M}}(h) - \frac{\omega h}{k_0^2}\frac{g'(h)}{g(h)}u_{\text{E}}(h), \\ p_{\text{M}}(h)u'_{\text{M}}(h) &= \gamma m\left(\frac{1}{k^2(h)} + \frac{1}{k_0^2}\right)u_{\text{E}}(h) - \frac{\omega h}{k_0^2}\frac{g'(h)}{g(h)}u_{\text{M}}(h), \end{aligned} \tag{5.5}$$

where function $g(\rho) = I_m(k_0\rho)$ or $g(\rho) = K_m(k_0\rho)$ are solutions outside or inside the ring as appropriate.

Summing up (5.3), (5.4) and substituting (5.5) for $p_{\text{E}}(h)u'_{\text{E}}(h)$, $p_{\text{M}}(h)u'_{\text{M}}(h)$, we obtain the variational equation

$$\begin{aligned} &\gamma m\left(\frac{1}{k^2(h)} + \frac{1}{k_0^2}\right)(u_{\text{M}}(h)v_{\text{E}}(h) + u_{\text{E}}(h)v_{\text{M}}(h)) - \frac{\omega h}{k_0^2}\frac{g'(h)}{g(h)}\big(u_{\text{E}}(h)v_{\text{E}}(h) \\ &\quad + u_{\text{M}}(h)v_{\text{M}}(h)\big) - \int_{h_0}^{h}\left(p_{\text{E}}u'_{\text{E}}v'_{\text{E}} + p_{\text{M}}u'_{\text{M}}v'_{\text{M}}\right)d\rho - \int_{h_0}^{h}\left(q_{\text{E}}u_{\text{E}}v_{\text{E}} + q_{\text{M}}u_{\text{M}}v_{\text{M}}\right)d\rho \\ &\quad - \int_{h_0}^{h} f\left(u_{\text{M}}v_{\text{E}} + u_{\text{E}}v_{\text{M}}\right)d\rho = 0, \end{aligned} \tag{5.6}$$

which hold for any test functions v_{E} and v_{M}. The solution of (5.6) is equivalent to the original problem P_m.

6 Projection method

Using the projection method [2] let us reduce the variational equation (5.6) to a system of algebraic equations. Firstly, split an interval $[h_0,\ h]$ into n subintervals with the length $l = |h_0 - h|/n$. Let us define a set of n subintervals

$$\Phi_i = [h_0 + (i-1)l,\ h_0 + (i+1)l],\ i = 1, ..., n-1,\ \ \Phi_n = [h_0 + (n-1)l,\ h]$$

and set of $n+1$ subintervals

$$\begin{aligned} &\Psi_1 = [h_0,\ h_0 + l], \quad \Psi_j = [h_0 + (i-2)l,\ h_0 + il],\ \ j = 2, ..., n, \\ &\Psi_{n+1} = [h_0 + (n-1)l,\ h]. \end{aligned}$$

These subintervals we call base finite elements. Denote by $a, b,$ and c an initial point, midpoint and endpoint of subintervals, respectively.

In accordance with the scheme of the projection method, it is necessary to introduce *basis functions* ϕ_i and ψ_j in order to approximate the solution. The basis functions are defined on each subinterval Φ_i and Ψ_j (ϕ_i and ψ_j vanishes outside the intervals Φ_i and Ψ_j, respectively).

The basis functions ϕ_i defined on Φ_i, are

$$\phi_i = \begin{cases} \dfrac{1}{b-a}(\rho - a), & \rho < b, \\ \dfrac{1}{b-c}(\rho - c), & \rho > b, \end{cases} \quad i = \overline{1, n-1}, \quad \phi_n = \frac{1}{c-a}(\rho - a).$$

The basis functions ψ_i defined on Φ_i are

$$\psi_1 = -\frac{1}{(c-a)^2}\left(\rho^2 - 2a\rho + a^2 - (c-a)^2\right),$$

$$\psi_2 = \begin{cases} \dfrac{1}{(c-a)^2}\left(\rho^2 - 2a\rho + a^2\right), & \rho < b, \\ \dfrac{1}{b-c}(\rho - c), & \rho > b, \end{cases} \quad \psi_j = \begin{cases} \dfrac{1}{b-a}(\rho - a), & \rho < b, \\ \dfrac{1}{b-c}(\rho - c), & \rho > b, \end{cases}$$

where $j = 3, ..., n$ and $\psi_{n+1} = \frac{1}{c-a}(\rho - a)$.

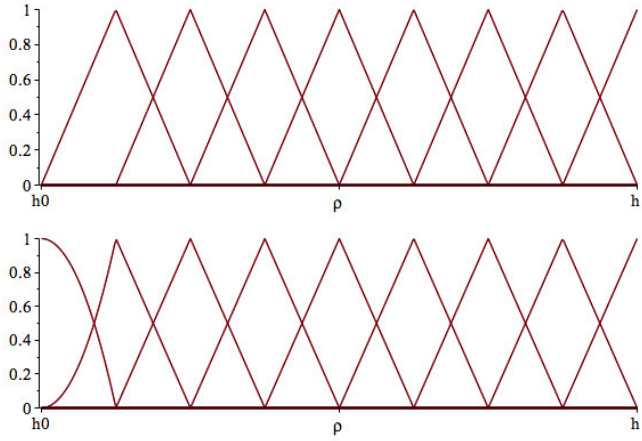

Figure 3. The basis functions ϕ_i and ψ_j, defined on $[h_0,\ h]$.

Such defined basis functions takes into account the physical nature of the problem under consideration (see Remark 2 and Figure 3).

We assume an approximate solution with real coefficients α_i and β_j such that

$$u_{\mathrm{E}} = \sum_{i=1}^{n} \alpha_i \phi_i, \quad u_{\mathrm{M}} = \sum_{j=1}^{n+1} \beta_j \psi_j. \tag{6.1}$$

Substituting functions u_{E} and u_{M} with representations (6.1) into the variational equation (5.6), we obtain a system of linear equations with respect to α_i and β_j (for fixed value of γ)

$$Ax = 0,$$

where matrices A and x have the form

$$A = \begin{pmatrix} A^{11}_{\text{EE}} & \cdots & A^{1n}_{\text{EE}} & A^{11}_{\text{EM}} & \cdots & A^{1,n+1}_{\text{EM}} \\ \vdots & \ddots & \vdots & \vdots & \ddots & \vdots \\ A^{n1}_{\text{EE}} & \cdots & A^{nn}_{\text{EE}} & A^{n1}_{\text{EM}} & \cdots & A^{n,n+1}_{\text{EM}} \\ A^{11}_{\text{ME}} & \cdots & A^{1n}_{\text{ME}} & A^{11}_{\text{MM}} & \cdots & A^{1,n+1}_{\text{MM}} \\ \vdots & \ddots & \vdots & \vdots & \ddots & \vdots \\ A^{n+1,1}_{\text{ME}} & \cdots & A^{n+1,n}_{\text{ME}} & A^{n+1,1}_{\text{MM}} & \cdots & A^{n+1,n+1}_{\text{MM}} \end{pmatrix}, \quad x = \begin{pmatrix} \alpha_1 \\ \vdots \\ \alpha_n \\ \\ \beta_1 \\ \vdots \\ \beta_{n+1} \end{pmatrix},$$

with elements

$$A^{ii}_{\text{EE}} = -\frac{\omega h}{k_0^2}\frac{g'(h)}{g(h)}\phi_i^2(h) - \int_{\Phi_i}\left(p_{\text{E}}(\phi_i')^2 + q_{\text{E}}\phi_i^2\right)d\rho,$$

where used $v_{\text{E}} = \phi_i$ and $i = 1, ..., n$;

$$A^{ij}_{\text{EM}} = \gamma m\left(\frac{1}{k^2(h)} + \frac{1}{k_0^2}\right)\phi_i(h)\psi_j(h) - \int_{\Phi_i} f\phi_i\psi_j d\rho,$$

where used $v_{\text{M}} = \psi_j$ and $i = 1, ..., n,\ j = 1, ..., n+1$;

$$A^{ji}_{\text{ME}} = \gamma m\left(\frac{1}{k^2(h)} + \frac{1}{k_0^2}\right)\phi_i(h)\psi_j(h) - \int_{\Psi_j} f\phi_i\psi_j d\rho,$$

where used $v_{\text{E}} = \phi_i$ and $i = 1, ..., n,\ j = 1, ..., n+1$;

$$A^{jj}_{\text{MM}} = -\frac{\omega h}{k_0^2}\frac{g'(h)}{g(h)}\psi_j^2(h) - \int_{\Psi_j}\left(p_{\text{M}}(\psi_j')^2 + q_{\text{M}}\psi_j^2\right)d\rho,$$

where used $v_{\text{M}} = \psi_j$ and $j = 1, ..., n+1$. Thus A is a $(2n+1)\times(2n+1)$ matrix. Let us denote by Δ the determinant of A

$$\Delta(\gamma) = \det A.$$

Remark 3. If there exists $\gamma = \widetilde{\gamma}$ such that $\Delta(\widetilde{\gamma}) = 0$, then $\widetilde{\gamma}$ is an approximate spectral parameter of Problem P_m. In other words, if an interval $[\underline{\gamma},\ \overline{\gamma}]$ is such that $\Delta(\underline{\gamma}) \times \Delta(\overline{\gamma}) < 0$, then this means that there exists $\gamma = \widetilde{\gamma} \in [\underline{\gamma},\ \overline{\gamma}]$ which is an spectral parameter of Problem P_m. This value can be calculated with any prescribed accuracy.

7 Numerical results

Numerical results are obtained with the help of the shooting method for GL (see Figure 1). For the inhomogeneity $\varepsilon(\rho)$ of the waveguide the following functions are used to specify the permittivities $\varepsilon = \varepsilon + \frac{\rho}{20}$ and $\varepsilon = \varepsilon_c + \frac{\rho-2}{2}$ in the layer $h_0 < \rho < h$, where ε_c is a positive real constant.

The dielectric constant determined by the expression $\varepsilon_c+\frac{\rho}{20}$ defines a weakly inhomogeneous medium, which can be compared with homogeneous. The function $\varepsilon_c + \frac{\rho-2}{2}$ defines a filling considerably different from the homogeneous waveguide.

In the figures below the profiles of dielectric permittivity, the spectral parameter γ with respect to angular parameter m and to angular frequency ω, and functions $\mathrm{E_z}$ and $\mathrm{H_z}$ are shown.

The following values of parameters are used for calculations in Figures 4–13: $\varepsilon_0 = 1$, $\varepsilon_c = 4$, $h_0 = 2$, and $h = 4$.

In Figures 4 and 5 are presented the permittivity profiles. The red and blue curves correspond to inhomogeneous and homogeneous waveguide structures.

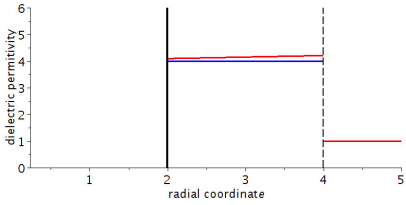

Figure 4. The profiles of dielectric permittivity: $\varepsilon_c + \frac{\rho}{20}$ (red curve) and ε_c (blue curve).

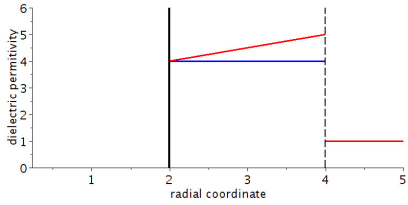

Figure 5. The profiles of dielectric permittivity: $\varepsilon_c + \frac{\rho-2}{2}$ (red curve) and ε_c (blue curve).

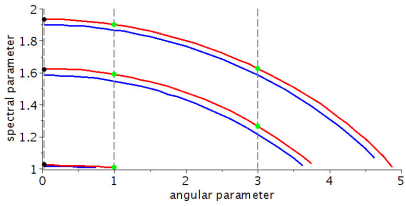

Figure 6. The dependence of spectral parameter γ with respect to m in case of $\omega = 1$. Red and blue colours corresponds to $\varepsilon_c + \frac{\rho}{20}$ and ε_c, respectively.

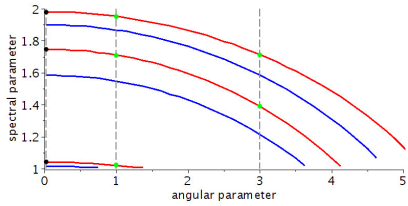

Figure 7. The dependence of spectral parameter γ with respect to m in case of $\omega = 1$. Red and blue colours corresponds to $\varepsilon_c + \frac{\rho-2}{2}$ and ε_c, respectively.

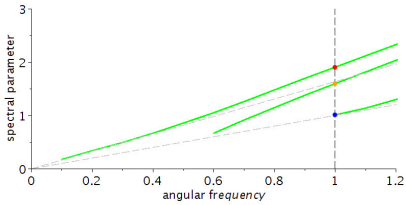

Figure 8. The dependence of spectral parameter γ with respect to frequency ω (dispersion curves) in case of $m = 1$. The permittivity is specified by $\varepsilon_c + \frac{\rho}{20}$.

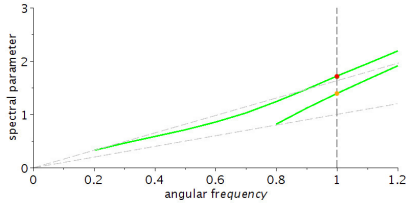

Figure 9. The dependence of spectral parameter γ with respect to frequency ω (dispersion curves) in case of $m = 3$. The permittivity is specified by $\varepsilon_c + \frac{\rho-2}{2}$.

Figures 6 and 7 are graphs of the spectral parameter depending on the angular parameter. The color of curves for the homogeneous and inhomogeneous waveguides coincides with the colors for the dielectric permittivity profiles in Figures 4 and 5. As one would expect the graphs of the homogeneous and weakly inhomogeneous waveguides differ only slightly.

Only integer values of the angular parameter m are physically meaningful. But we can investigate this problem numerically for any values of the angular parameter m (for non-integer, too). When m is equal to 0, the problem splits into two well-studied problem - propagation of TE and TM polarized waves. In these, the first and third black dots correspond to the spectral parameters of the TM waves, where as the second black dot is the spectral parameter of TE waves. These graphs show the connection between the TE and TM waves ($m = 0$) and hybrid waves ($m \neq 0$).

For the value of the angular parameter m equal to 1 and 3, the dispersion curves were plotted in Figures 8 and 9. The interior of the dashed region determines the area of the parameter space where the homogeneous problem has a solution.

For the value of the frequency $\omega = 1$ the graphs of the tangential components E_z and H_z of the electromagnetic field in Figures 10–13 are presented. Color of curves in Figures 10–13 corresponds to the color of spectral parameter in Figures 8 and 9 (points of intersections of vertical dashed line with the dispersion curves).

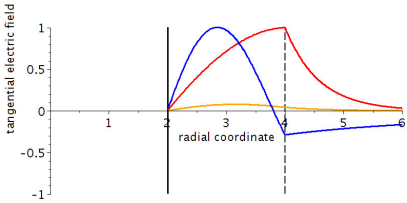

Figure 10. The tangential components E_z of electric field in case of $m = 1$, $\omega = 1$. The permittivity is specified by $\varepsilon_c + \frac{\rho}{20}$.

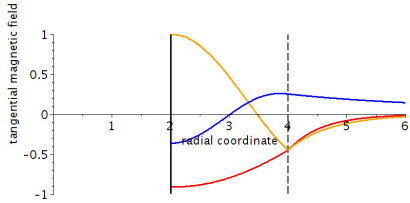

Figure 11. The tangential components H_z of electric field in case of $m = 1$, $\omega = 1$. The permittivity is specified by $\varepsilon_c + \frac{\rho}{20}$.

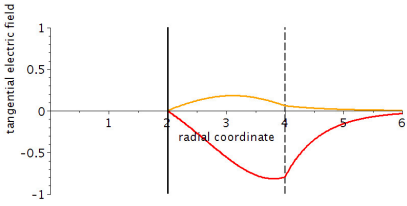

Figure 12. The tangential components E_z of electric field in case of $m = 3$, $\omega = 1$. The permittivity is specified by $\varepsilon_c + \frac{\rho-2}{2}$.

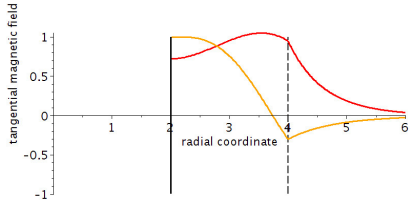

Figure 13. The tangential components H_z of electric field in case of $m = 3$, $\omega = 1$. The permittivity is specified by $\varepsilon_c + \frac{\rho-2}{2}$.

Graphs of the tangential components of the electromagnetic field (Figures 10–13) consistent with the physical formulation of the problem, namely the component E_z vanishes on the boundary of the metal, both of components E_z and H_z are continuous at the interface and decays when $\rho \to \infty$.

8 Conclusions

The propagation of monochromatic electromagnetic waves in metal circular cylindrical dielectric waveguides filled with inhomogeneous medium was considered. By applying methods of the theory of integral operators, we gave a rigorous mathematical description of the problem, substantiated and implemented a numerical method for its solution.The method allows us to determine approximate eigenvalues with any prescribed accuracy. The approach described in this paper can be applied to other problems, e.g., to multilayered opened waveguides.

Acknowledgements

The author is grateful to Yu.G. Smirnov for useful discussions and attention to the study. This study is supported by the Ministry of Education and Science of the Russian Federation, Project No. 1.894.2017/П.

References

[1] J.C. Baumert and J. Hoffnagle. Numerical method for the calculation of mode fields and propagation constants in optical waveguides. *Journal of Lightwave Technology*, **4**(11):1626–1630, 1986. https://doi.org/10.1109/JLT.1986.1074671.

[2] D. Colton and R. Kress. *Integral Equation Methods in Scattering Theory*. Wiley, New York, 1984.

[3] C.R. Doerr and H. Kogelnik. Dielectric waveguide theory. *Journal of Lightwave Technology*, **26**(9):1176–1187, 2008. https://doi.org/10.1109/JLT.2008.923632.

[4] G. Lifante, F. Cusso and E. Cantelar. Numerical methods for optical waveguide devices. In *2006 International Conference on Mathematical Methods in Electromagnetic Theory*, pp. 77–82. Mathematical Methods in Electromagnetic Theory, 2006 International Conference on, 2006. https://doi.org/10.1109/MMET.2006.1689711.

[5] A.F. Nikiforov and V.B. Uvarov. *Special Functions of Mathematical Physics*. Nauka, Moscow, 1978.

[6] S.M. Saad. Review of numerical methods for the analysis of arbitrarily-shaped microwave and optical dielectric waveguides. *IEEE Transactions on Microwave Theory and Techniques*, **33**(10):894–899, 1985. https://doi.org/10.1109/TMTT.1985.1133147.

[7] A.S. Silbergleit and Yu.I. Kopilevich. *Spectral theory of guided waves*. Institute of Physics Publish., Bristol and Philadelphia, 1996.

[8] E. Smolkin and Y. Shestopalov. Numerical analysis of electromagnetic wave propagation in metal-dielectric waveguides filled with nonlinear medium. In *2016 Progress in Electromagnetic Research Symposium (PIERS)*, pp. 222–226, 2016. https://doi.org/10.1109/PIERS.2016.7734297.

[9] E. Smolkin and Y. Shestopalov. Numerical study of multilayered nonlinear inhomogeneous waveguides in the case of TE polarization. In *2016 10th European Conference on Antennas and Propagation (EuCAP)*, pp. 1–5. Antennas and Propagation (EuCAP), 2016 10th European Conference on, 2016. https://doi.org/10.1109/EuCAP.2016.7481782.

[10] E.Y. Smolkin. Goubau line filled with nonlinear medium: Numerical study of TM-polarized waves. In *2015 International Conference on Electromagnetics in Advanced Applications (ICEAA)*, pp. 1572–1575, 2015. https://doi.org/10.1109/ICEAA.2015.7297390.

[11] A.W. Snyder and J. Love. *Optical waveguide theory*. Springer US, 1983.

[12] M.S. Sodha and A.K. Ghatak. *Inhomogeneous Optical Waveguides*. Springer, US, 1977. https://doi.org/10.1007/978-1-4615-8762-0.

[13] A. Sommerfeld. Ueber die Fortpflanzung elektrodynamischer Wellen längs eines Drahtes. *Annalen der Physik*, **303**(2):233–290, 1899. https://doi.org/10.1002/andp.18993030202.

[14] L.A. Vainshtein. *Electromagnetic Waves*. Radio i Svyaz, Moscow, 1988. (in Russian)

[15] R.K. Varshney, I.C. Goyal and A.K. Ghatak. A simple and efficient numerical method to study propagation characteristics of nonlinear optical waveguides. *Journal of Lightwave Technology*, **16**(4):697–702, 1998. https://doi.org/10.1109/50.664085.

[16] G.I. Veselov and S.B. Raevskii. *Layered Metal-Dielectric Waveguides*. Radio i Svyaz, Moscow, 1988. (in Russian)